Supplementary Information

MoS_2-modified Curcumin Nanostructures: The Novel Theranostic Hybrid having Potent Antibacterial and Antibiofilm activities against Multi-Drug-Resistant Hypervirulent *Klebsiella pneumoniae*

Ashish Kumar Singh[1, 2¶], Himanshu Mishra[3¶], Zeba Firdaus[4¶], Shivangi Yadav[1¶], Prerana Aditi[4], Nabarun Nandy[5], Kavyanjali Sharma[6], Priyanka Bose[7], Akhilesh Kumar Pandey[2], Brijesh Singh Chauhan[2], Kaushik Neogi[8], Kunwar Vikram[9], Anchal Srivastava[3], Amrita Ghosh Kar[6], Pradyot Prakash[1*]

[1]Bacterial Biofilm and Drug Resistance Research Laboratory, Department of Microbiology, Institute of Medical Sciences, Banaras Hindu University, Varanasi 221005, India.
[2]Department of Biochemistry, Institute of Science, Banaras Hindu University, Varanasi 221005, India.
[3]Nano Research Laboratory, Department of Physics, Institute of Science, Banaras Hindu University, Varanasi 221005, India.
[4]Department of Medicinal chemistry, Institute of Medical Science, Banaras Hindu University, Varanasi 221005, India
[5]Cytogenetics Laboratory, Department of Zoology, Institute of Science, Banaras Hindu University, Varanasi 221005, India.
[6]Department of Pathology, Institute of Medical Sciences, Banaras Hindu University, Varanasi 221005, India.
[7]Department of Chemistry, Institute of Science, Banaras Hindu University, Varanasi 221005, India.
[8]Department of Pharmaceutical Engineering and Technology, Indian Institute of Technology, Banaras Hindu University, Varanasi 221005, India.

[9]Department of Physics, Indian Institutes of Sciences, Bangalore 560012, India and Graphic Era University, Dehradun 248002, India

[¶]These authors have contributed equally

***E-mail: pradyot_micro@bhu.ac.in, Contact: +91-9453311721**

Supplementary information 1

Synthesis of MoS_2-QDs

Functionalized molybdenum disulfide quantum dots (MoS_2-QDs) have been synthesized using facile, single step and eco-friendly hydrothermal route. Sodium molybdate dihydrate ($Na_2MoO_4.2H_2O$) and L-cysteine ($C_3H_7NO_2S$) have been used as starting materials. 0.25 g of sodium molybdate and 0.5 g of L-cysteine have been dissolved into two beakers containing 25 ml and 50 ml DI water separately followed by stirring for 10 minute at 40 ºC. After that, both the solutions are mixed together with pH adjustment ~5 using 0.1 M HCl. Final solution has been transferred into a stainless steel lined Teflon autoclave having capacity 100 ml and tightly sealed. Autoclave was put inside an oven maintained at 220°C for hydrothermal reaction for 36 hours. After the completion of reaction light yellowish solution containing MoS_2-QDs has been taken out for the further studies.

Characterization of MoS_2-QDs

Figure S1 (a) shows the TEM image of MoS_2-QDs (encircled with red color). Size of the MoS_2-QDs varies from ~2 nm to ~6 nm. Raman spectra of MoS_2-QDs as well as its bulk counterpart has been shown in figure S 1(b). It can be seen that for bulk MoS_2 structure two clearly distinct Raman peaks are observed at positions ~381.37 cm^{-1} and 406.13 cm^{-1}. These two Raman peaks are assigned to the in-plane vibration and out of plane vibration of Mo and S atoms and named as E^1_{2g} and A_{1g} respectively. For bulk MoS_2, wavenumber difference between E^1_{2g} and A_{1g} is found to be 24 cm^{-1}. For MoS_2-QDs, we did not get any Raman peak may be due to the fluorescing nature of QDs or amorphous structure. Absorption spectrum of MoS_2-QDs show a strong band at ~388 nm corresponding to its excitonic transition. Excitation dependent PL spectra of MoS_2-QDs has been

shown in the figure S1(d) which shows a broad emission range from ~350 nm to 600 nm. This broad PL of MoS_2-QDs may be attributed to polydispersity of particles.

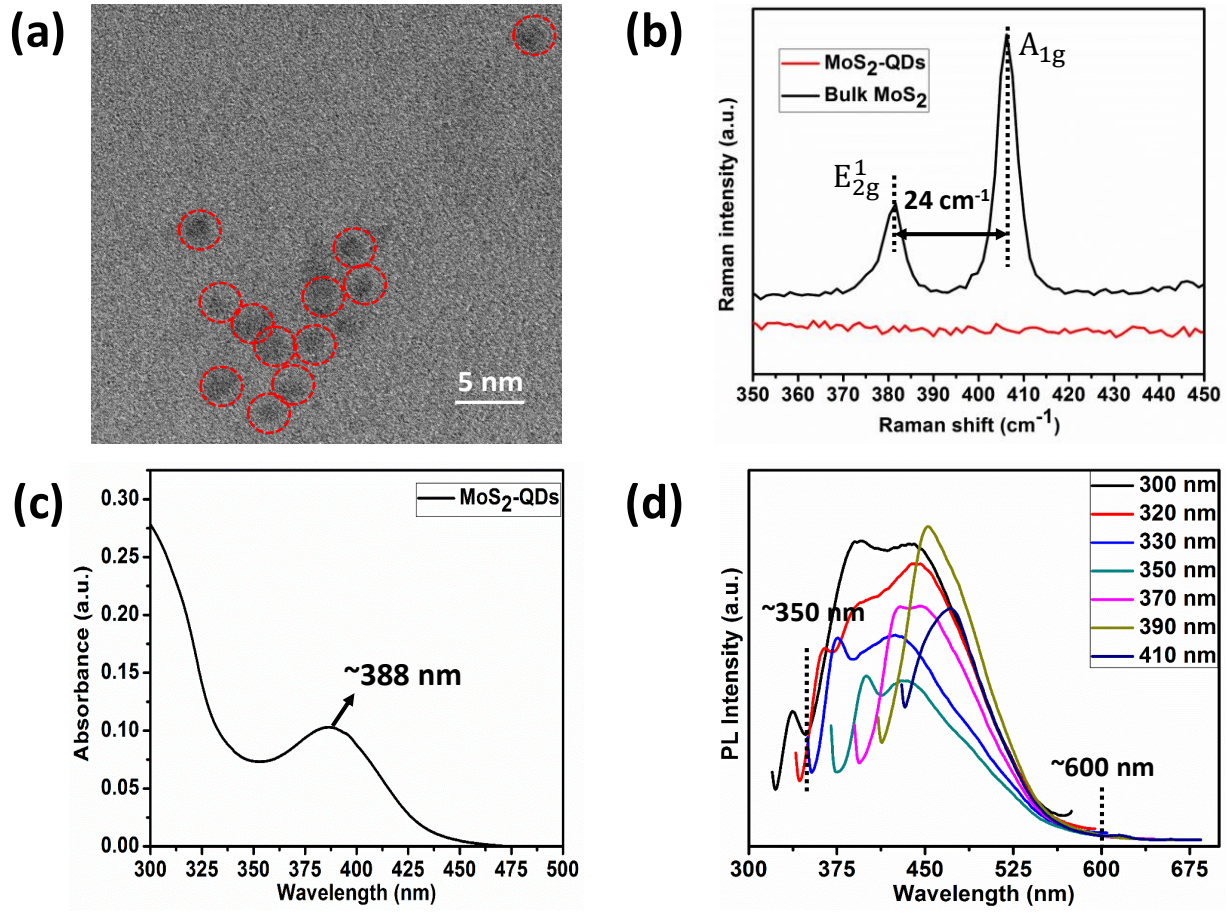

Figure S1 (a) TEM images of MoS_2-QDs, (b) Raman spectra of MoS_2-QDs as well as its bulk counterpart, (c) UV-vis absorption spectra and (d) excitation dependent PL of MoS_2-QDs.

Figure S2 (a) shows the PL spectra of MQC with an excitation wavelength ~663 nm (Laser excitation wavelength used in Raman spectrometer). Under laser excitation, MQC gives a broad emission with a kink present at 1.83 eV which corresponds to the band gap of MoS_2. As it has been already discussed in the main manuscript that with an excitation wavelength ~663 nm Laser

excitation, no Raman signal corresponding to CurQDs was obtained for higher wavenumber range ($\geq$ 1000 cm^{-1}). This could be explained as follows:

When the MQC sample is excited with excitation wavelength ~663 nm (= 1.87 eV), it goes to a Raman virtual level (figure S2(b)). From where it relaxes to the conduction band of MoS_2-QDs through non-radiative process. Finally from the conduction band of MoS_2-QD it goes to the ground state of valence band of MoS_2-QDs through radiative process and hence yield a photon equal to its band gap (= 1.83 eV). This is the reason for the observation of a kink at ~1.83 eV in the emission spectrum of MQC at excitation wavelength ~663 nm. From the absorption spectra of CurQDs (figure 3(a)), it can be seen that the presence of absorption band at ~427 nm corresponds to ~2.91 eV of energy gap. Here we are exciting the sample with an excitation source corresponding to ~1.87 eV energy, which matches well with the band gap of MoS2-QDs, and hence fluorescence for MoS_2-QDs dominates irrespective to the Raman signal of CurQDs. Therefore, to obtain the Raman signal corresponding to CurQDs one should excite the MQC sample with an excitation source having energy less than the band gap of MoS_2-QDs i.e. ~1.87 eV. This was proved in our earlier report where Raman spectra of CurQDs have been recorded with an excitation wavelength of ~785 nm.

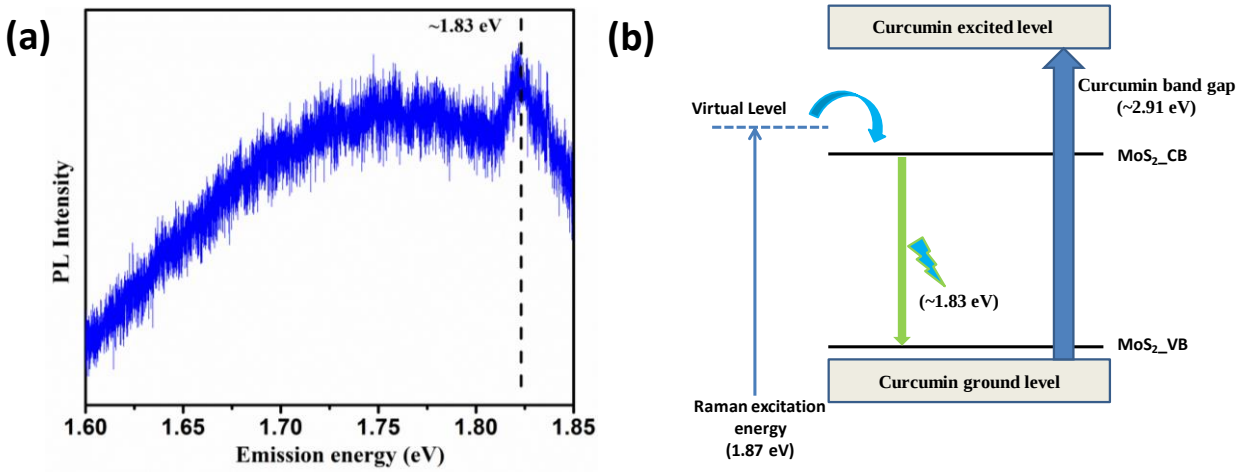

Figure S2 (a) Fluorescence due to MQC excited with 663 nm Laser equipped in Raman spectrometer and (b) schematic diagram explaining the fluorescence arising in MQC while doing Raman characterization with a ~663 nm excitation Laser source equipped within Raman spectrometer.

Table S1: The fitted data for time resolved photoluminescence with decay time and chi square

	Decay time (ns)		**Fitting constants**	**% Contribution**	χ^2
τ_1	0.10 ± 0.005	B_1	0.455 ± 0.0141	47.09	
τ_2	0.70 ± 0.1224	B_2	0.021 ± 0.0021	14.77	1.41
τ_3	1.72 ± 0.0610	B_3	0.0026 ± 0.0002	38.14	

Quantum yield calculation:

Quantum yield (QY) of MoS_2-QDs and MQC samples have been calculated considering quinine sulfate (QY = 0.546) as the reference. The following equation has been used for the calculation:

$$QY = QY_r \left(\frac{OD_r}{I_r} \text{ X } \frac{1}{n_r^2}\right) \left(\frac{In^2}{OD}\right)$$

Here, QY_r = quantum yield of the reference i.e. quinine sulfate;

n = refractive index of solvents used for sample;

n_r = refractive index of solvents used for reference solutions;

OD_r and OD = optical densities of the reference and sample wavelength 308 nm;

I and I_r = integrated intensities of the sample and reference PL spectra respectively.

The solvent for dissolving Quinine Sulfate has been used was 0.1 M H_2SO_4 (n_r = 1.63) and for *f*-MoS_2-QDs is DI water (n = 1.33) as depicted in the table below:

Table S2: Quantum yield (QY) of MoS_2-QDs and MQC with respect to quinine sulfate (QY = 0.546)

Sample	**Integrated emission intensity (I)**	**Absorbance at 308 nm**	**Refractive index of solvent (η)**	**Quantum Yield (QY)**
Quinine Sulfate	38907.6	0.0134	1.63	0.546 (Known)
MoS_2-QDs	3582.0	0.0150	1.33	0.0299
MQC	17476.6	0.0811	1.33	0.0271

Supplementary information 2:

FTIR-ATR of MQCs:

Bare MoS_2 showed strong and broad absorption peak around 482 cm^{-1}, which is the characteristic of MoS_2 bond. The peak at 482 cm^{-1} in MoS_2 shifted to 502 cm^{-1} in MQCs and was less pronounced suggesting the presence of an altered MoS_2-O bond due to its interaction with curcumin. The frequency region of both phenolic ϑ(OH) vibrations of the curcumin was computed to be at 3435 cm^{-1}, but was shifted to lower frequency at 3348 cm^{-1} due to intramolecular and intermolecular H-bonding in curcumin. In MQCs, no band shifting was noted (3445 cm^{-1}) indicating negligible interaction of these phenolic hydroxyls with MoS_2. A plethora of literature suggests that the phenolic hydroxyl group of curcumin is not involved in complexation with other metals exhibiting unaltered vibrational band around 3200-3500 cm^{-1}.The β-diketone group at the center is the salient feature of curcumin, which has potentially high driving force for metal chelation. Recently, the β-diketo system in curcumin was reported to form charge transfer complexes with TiO_2 nanoparticles. Another report based on MS (mass spectral) data by Khalil *et al.* suggests a four-coordination zinc-curcumin complex through β-diketo system. This could be due to the co-existence of keto and enol groups in curcumin molecules. In this regard, it is not surprising that β-diketone moiety has possibly interacted with Mo atom at the bulk surface of MoS_2. Some reports suggest that the curcumin spectra did not exhibit any peak in the carbonyl region (1800–1650 cm^{-1}) indicating that curcumin exists mainly in the enol form. However, we noted a peak in this region at ~ 1661 cm^{-1} for the MQCs, which may be the indicative of peak arising due to ϑ(C=O) stretching of curcumin. Theoretical calculations show that the enolic ϑ(OH) mode of curcumin appears at 2979 cm^{-1}. Experimentally, this band usually appears weak and broad. The absence of a clearly defined ϑ(OH) band has been explained by Tayyari *et al.* as a function of the strength of the

intramolecular hydrogen bond which decreases its intensity and increase its broadness. They further suggested that the π-systems like phenyl groups increase the strength of H-bond through conjugation with the enol ring. In our case, the hydroxyl and methoxy groups on the phenyl rings of curcumin are electron-donating groups, which further strengthen the hydrogen bond. Therefore, if the electronegativity of these groups is somehow decreased by forming bonds or conjugation with other moieties would weaken the hydrogen bond strength and thus allow the enol peak to appear more clearly. In our present study, we observed a band at 2995-96 cm^{-1} for MQCs. However, the appearance of the said prominent enol peak may also be due to chelation of MoS_2 with curcumin as suggested earlier for zinc-curcumin complex. In curcumin, another prominent band appeared at 1514 cm^{-1} which was due to highly mixed vibrations of ϑ(C=O), δ(CC=O), and δ(CCC). The IR bands in frequency region 1410–1450 cm^{-1} were due to deformation vibrations of the two-methyl groups. In complexes the bands due to C=O stretching should be shifted to lower frequencies during complexation. IR spectrum of curcumin showed ϑ(C=O) at 1642 cm^{-1}, which shifted to higher energy when complexed with MoS_2 at 1661 cm^{-1} indicative of a relatively strong coordination of the carbonyl moiety due to chelation with MoS_2. This could also be supported by the disappearance (at 950 cm^{-1}) and shifting (at 897 cm^{-1}) of the IR bands respectively in MQCs, which are attributed to ϑ(C–O) vibrations. The present spectroscopic analysis supports that curcumin chelates with MoS_2. These peak shiftings are due to formation of co-ordinate bonds between Molybdenum atom and the electron rich β-diketo centre showing the keto-enol tautomerism.

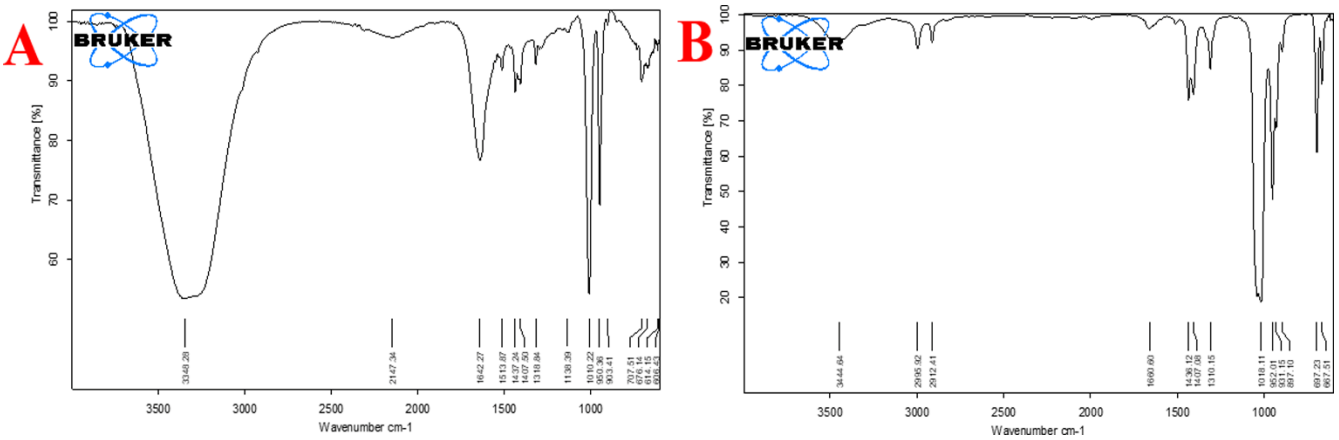

Panel A: FTIR-ATR of Curcumin dissolved in DMSO and diluted in water

Panel B: FTIR-ATR of MQCs

Supplementary information 3:

***In vivo* evaluation of cytotoxicity:**

Biochemical Profiling from serum and tissues:

The whole blood (~1.7 ml) of the sacrificed rats was collected in EDTA (Ethylene diamine tetra acetic acid) blood collecting vials. To separate serum, the clotted blood was spun at 3000 rpm for 20 mins, which was assayed for alanine aminotransferase (ALT), aspartate aminotransferase (AST) and), glucose, alanine aminotransferase, aspartate aminotransferase, creatinine, and urea using colorimetric assay kits procured from Accurex Biomedical, India. Total haemoglobin was also estimated using Haemocor D kit. SOD and catalase assays were performed manually for serum. Analysis of blood element viz. red blood cell counts (RBCs), white blood cells (WBCs), mean corpuscular hemoglobin concentration (MCHC), platelet count (PLT), mean corpuscular hemoglobin (MCH), mean corpuscular volume (MCV) and hematocrit (HCT) were carried out using hematological auto analyzer (MS-9-3 France). Lipid peroxidation, superoxide dismutase activity, and catalase activity were assayed on liver and kidney tissues.

Protein estimation

We estimated the total protein concentration by Bradford method using bovine serum albumin (BSA) as standard described elsewhere.[25] Briefly, BSA was dissolved in DI water in a range of dilutions for the calibration curve, and 10 µl of the separated supernatant (from the tissue homogenate as well as serum) was dispensed in TCP wells. To those wells, 200 µl of the diluted Bradford reagent was added and incubated for 20 mins at room temperature. The absorbances were measured at 595nm employing Synergy H1 Hybrid Multi-Mode Reader. The procedure was performed in triplicate for each sample.

Lipid peroxidation assay

The malondialdehyde content, a measure of lipid peroxidation, was assayed in the form of thiobarbituric acid-reactive substances (TBARS) by the method described earlier with modifications.[26] Briefly, to 500 µl of supernatant (obtained from the tissue homogenate) the same volume of 10% trichloroacetic acid (500 µl) was added and centrifuged at 1,000 X g for 10 min. To 500 µl of thus obtained supernatant, an equal volume of 50% glacial acetic acid and 1 ml of 0.67% thiobarbituric acid were added with subsequent incubation for 15 mins in boiling water bath. After cooling, absorbance was measured at 532 nm. Thiobarbituric acid-reactive substances were quantified using an extinction coefficient of 1.56 X 105 M^{-1} cm^{-1} and expressed as nanomole of malondialdehyde per milligram protein.

Superoxide dismutase assay:

It was done by using the method described by Beauchamp and Fridovich.[27] Three tubes were prepared namely sample tube(s), control tube, and blank. Reaction mixture in sample tube contained SOD buffer (pH 7.8), 130mM L-methionine (300 µl), 10 times diluted homogenate (250 µl), 750µM Nitroblue tetrazolium chloride (NBT, 150µl), 0.5mM EDTA (75µl) and 60µM riboflavin (100 µl). The control tube was devoid of homogenate while riboflavin was not added in the blank tube. The tubes were kept in front of fluorescent light for 10 min. NBT gets reduced by a photochemical reaction in presence of riboflavin under fluorescent light and formed a blue color product formazan. In presence of the enzyme, the reaction was inhibited to a different extent depending on the activity of the enzyme and the color produced was read at 560 nm.

Catalase assay

Catalase activity was assessed by monitoring the rate of decomposition of H_2O_2 as reported earlier.[28] In brief, the reaction mixture contained 900 µl of 50mM catalase buffer (pH 7.0) and 100 µl-diluted homogenate was added to make volume 1 ml. The reaction was initiated by the addition of 30mM hydrogen peroxide (H_2O_2) and absorbance was measured at 240 nm for 3 min. Enzyme activity expressed in terms of µ mole/min/mg protein.

Table S3. Body weight indices of control and test group rats. Data represent (mean ± S.D.) (n=6).

Group	Initial body weight (gm)	Body weight after 48 hrs. (gm)	Body weight on day14 (gm)
Group I	105 ± 4.47	105 ± 7.1	130.8± 3.76
Group II	108.2 ± 5.9	100 ± 5.0	110.8± 5.85
Group III	105.8 ± 4.92	105 ± 7.1	132.2 ± 1.5
Group IV	101.7 ± 4.08	105 ± 7.1	129.2 ± 4.4
Group V	103.3 ± 5.16	115 ± 7.1	134.5 ± 3.94
Group VI	106.7 ± 5.16	110 ± 5.6	128.8 ± 7.36

Table S4: Vital organ indices and Organ/body weight ratio of different groups on 15th day. Data represent (Mean ± S.D.) (n=6).

Groups	**Liver (gm)**	**Liver/ Body weight ratio**	**Kidney (left) (gm)**	**Kidney/ Body weight ratio**	**Spleen (gm)**	**Spleen/ Body weight ratio**
Group I	5.09 ± 0.26	0.03890 ± 0.002	0.46 ± 0.027	0.0035 ± 0.0003	0.43 ± 0.014	0.00328 ± 0.00012
Group II	3.27 ± 0.23	0.0295 ± 0.0019	0.31 ± 0.014	0.0028 ± 0.0001	0.29 ± 0.014	0.00261 ± 0.00016
Group III	5.14 ± 0.15	0.0388 ± 0.001	0.44 ± 0.025	0.0033 ± 0.0002	0.41 ± 0.017	0.0031 ± 0.00012
Group IV	4.51 ± 0.3	0.0349 ± 0.002	0.42 ± 0.047	0.0032 ± 0.0004	0.39 ± 0.035	0.00301 ± 0.00017
Group V	5.4 ± 0.11	0.0401 ± 0.0008	0.46 ± 0.021	0.0034 ± 0.0002	0.42 ± 0.018	0.00312 ± 0.00014
Group VI	5.1 ± 0.5	0.0395 ± 0.0018	0.39 ± 0.067	0.0030 ± 0.0002	0.40 ± 0.039	0.0031 ± 0.00036

Table S5: Kit based serological profiling of control and test group rats. Data represent (Mean ± S.D.) (n=6).

Parameters	**Group I**	**Group II**	**Group III**	**Group IV**	**Group V**	**Group VI**
Glucose (mg/ml)	100.9 ± 10.6	116.5 9.5	101.7 ± 12.5	103.6 ± 11.9	102.7 ± 12.2	106.6 ± 9
GPT (U/L)	107.4 ± 7.8	140.3± 5.02	110.7 ± 6.4	107.6 ± 7.4	110.5 ± 7.3	112.1 ± 6.4
GOT (U/L)	70.2 ± 6.5	89.07 ± 4.5	68.3 ± 8	70 ± 4.2	66.9 ± 8.2	67 ± 3.8
SOD (U/mg protein)	2.07 ± 0.12	1.27 ±0.175	2.03 ± 0.15	2.01 ± 0.17	2.01 ± 0.15	2.06 ± 0.17
Catalase (U/mg protein)	20.25 ±1.32	14.57 ± 2.8	20.1 ± 1.83	19.85 ±1.57	21.5 ± 2.6	21.1 ± 2.34
Hemoglobin(g/dl)	12.07 ±0.55	10.26 ± 0.27	12.15 ± 0.46	12.43 ± 0.71	12.36 ± 0.82	12.21 ± 0.34
Urea (mg/dl)	45.9 ± 9.7	61.5 ± 5.2	43.27 ± 8.2	43.9 ± 8.2	45.2 ± 9.4	43.9 ± 6.7
Creatinine (mg/dl)	0.4 ± 0.014	0.65 ± 0.016	0.401 ± 0.17	0.402 ± 0.25	0.405 ± 0.28	0.403 ± 0.36

Table S6: Automated hematological profiling of control and test group rats. Data represent (Mean ± S.D.) (n=6).

Groups	**Hb (gm dl^{-1})**	**RBC (10^3 UL^{-1})**	**WBC (10^3 UL^{-1})**	**PLT (10^3 UL^{-1})**	**HCT (%)**	**MCHC (%)**	**MCH (pgm)**	**MCV (FI)**
Group-I	11.67 ± 0.64	8.28 ± 0.57	4.39 ± 0.75	5.14 ± 0.26	35.98 ± 1.08	33.9 ± 0.61	15.12 ± 0.55	45.6 ± 1.04
Group-II	9.77 ± 0.43	6.86 ± 0.78	3.67 ± 0.18	4.05 ± 1.12	32.25 ± 1.37	31.53 ± 0.72	12.9 ± 0.71	42.79 ± 1.62
Group-III	12.68 ± 0.71	8.25 ± 0.59	4.35 ± 0.24	5.08 ± 0.31	36.12 ± 0.54	33.78 ± 0.27	15.04 ± 0.26	46.04 ± 0.97
Group-IV	12.03 ± 0.66	8.21 ± 0.32	4.32 ± 0.13	4.92 ± 0.21	36.01 ± 1.10	34.04 ± 0.93	15.21 ± 0.24	45.81 ± 1.75
Group-V	11.94 ± 0.34	8.17 ± 0.21	4.27 ± 0.41	4.83 ± 0.17	36.37 ± 0.84	34.21 ± 0.46	15.13 ± 0.51	45.93 ± 0.87
Group-VI	11.86 ± 0.27	8.15 ± 0.13	4.21 ± 0.46	4.75 ± 0.35	36.15 ± 0.65	33.56 ± 0.25	15.07 ± 0.84	45.77 ± 0.39

Table S7: Protein estimation from liver, kidney, and serum among different groups of rats. Each experiment was done in triplicate. Data represents Mean±SD; n=6

Protein (mg/ml)	**Group I**	**Group II**	**Group III**	**Group IV**	**Group V**	**Group VI**
Liver	4.950± 0.0871	4.520±0.1716	4.222±0.0752	4.422±0.1837	4.018±0.1668	4.688±0.1155
Kidney	7.538±0.04401	7.335±0.1290	7.085±0.06950	7.012±0.05845	7.477±0.1553	7.368±0.04070
Serum	5.557±0.2541	4.550±0.2811	5.443±0.2714	5.460±0.3250	5.480±0.3382	5.433±0.2251

Table S8: Activities of enzymes in liver and kidney tissues respectively (A) lipid peroxidation as the level of TBARS/ MDA concentration (B) activity of superoxide dismutase (C) activity of catalase in various groups of rats. Each experiment was done in triplicate. Data represents Mean±SD; n=6

Groups	Parameters					
	Lipid Peroxidation*		Superoxide dismutase$		Catalase#	
	Liver	Kidney	Liver	Kidney	Liver	Kidney
Group I	0.7238±0.03215	0.4968±0.01396	3.020±0.1739	1.957±0.05071	325.8±5.211	133.3±3.958
Group II	0.8745±0.04183	0.5427±0.01860	2.340±0.09108	1.623±0.1341	291.5±19.39	99.85±7.094
Group III	0.7460±0.03579	0.4918±0.02157	3.033±0.1414	2.044±0.05091	334.9±7.477	130.1±7.764
Group IV	0.7237±0.02595	0.5088±0.02331	2.996±0.1456	2.038±0.02184	329.7±14.06	135.8±5.011
Group V	0.7507±0.04973	0.4906±0.01892	2.966±0.1155	2.069±0.05378	336.9±5.735	125.7±2.358
Group VI	0.7098±0.02168	0.4794±0.01609	3.015±0.1736	2.041±0.01895	326.0±8.475	128.6±8.704

*nM/mg protein, $µmole/min/mg protein, #µmole/min/mg protein